

# Quantum Plasmonics: Nonlinear Effects in the Field Enhancement of a Plasmonic Nanoparticle Dimer

D.C. Marinica,<sup>†</sup> A.K. Kazansky,<sup>‡,§</sup> P. Nordlander,<sup>||</sup> J. Aizpurua,<sup>⊥</sup> and A. G. Borisov<sup>\*,†</sup>

<sup>†</sup>Institut des Sciences Moléculaires d'Orsay, UMR 8214 CNRS-Université Paris-Sud, Bâtiment 351, 91405 Orsay Cedex, France

<sup>‡</sup>Material Physics Center CSIC-UPV/EHU and Donostia International Physics Center DIPC, Paseo Manuel de Lardizabal 4, 20018 Donostia-San Sebastián, Spain

<sup>§</sup>IKERBASQUE, Basque Foundation for Science, 48011, Bilbao, Spain

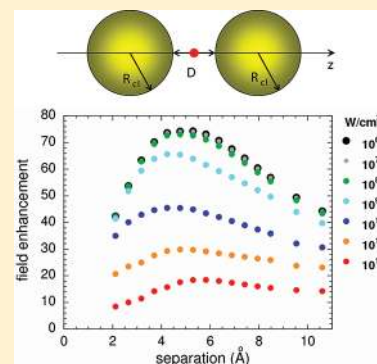
<sup>||</sup>Department of Physics and Astronomy, M.S. 61 Laboratory for Nanophotonics, Rice University, Houston, Texas 77251-1892, United States

<sup>⊥</sup>Material Physics Center CSIC-UPV/EHU and Donostia International Physics Center DIPC, Paseo Manuel de Lardizabal 5, 20018 Donostia-San Sebastián, Spain

## Supporting Information

**ABSTRACT:** A fully quantum mechanical investigation using time-dependent density functional theory reveals that the field enhancement in a coupled nanoparticle dimer can be strongly affected by nonlinear effects. We show that both classical as well as linear quantum mechanical descriptions of the system fail even for moderate incident light intensities. An interparticle current resulting from the strong field photoemission tends to neutralize the plasmon-induced surface charge densities on the opposite sides of the nanoparticle junction. Thus, the coupling between the two nanoparticles and the field enhancement is reduced as compared to linear theory. A substantial nonlinear effect is revealed already at incident powers of  $10^9$  W/cm<sup>2</sup> for interparticle separation distances as large as 1 nm and down to the touching limit.

**KEYWORDS:** Nanoparticle dimer, quantum plasmonics, field enhancement, nonlinear effects



Metal nanoparticle plasmonics is a fast-growing field of research due both to significant advances in experimental fabrication techniques and theoretical descriptions of the underlying phenomena. Collective excitation of the valence electrons by the incident electromagnetic field, the localized plasmon, leads to strong local field enhancement.<sup>1–5</sup> This opens a route to numerous practical applications, such as surface enhanced Raman scattering (SERS),<sup>6–8</sup> and optical nanoantennas<sup>9,10</sup> allowing, for example, the control of radiation from single quantum emitters<sup>11</sup> or generation of extreme ultraviolet pulses by nonlinear high harmonic generation.<sup>12</sup> In this context, the hybridization of plasmonic modes in nanoparticle assemblies can be used for rational engineering of plasmonic structures with desired optical response and local field profile. A prototypical geometry for plasmonic nanoparticle coupling, which has been widely considered in the literature is the plasmonic dimer.<sup>2–4</sup> Theoretical studies of this system based on the solution of the classical Maxwell equations where the nanoparticles are modeled with sharp surfaces predict extremely large fields in the nanoscale junction for small nanoparticle separations.<sup>3–8,13–16</sup> This is because of the high charge densities induced at the opposite sides of the junction at plasmon resonance.

However, recent calculations have shown that several factors can severely limit the field enhancement in a realistic system.

Indeed, for very narrow junctions, quantum mechanical effects start to be important.<sup>17</sup> These are primarily (i) the spill out of electrons outside the nanoparticle surfaces and electron tunneling across the junction, (ii) the finite spatial profile of the plasmon-induced screening charge.<sup>18</sup> The latter effect can be included in a classical description using spatially nonlocal dielectric functions.<sup>2,19–21</sup> However, this approach neglects electron tunneling across the junction so that it is limited to interparticle distances where the electronic densities of nanoparticles do not overlap. To properly account for both effects (i) and (ii), one therefore needs a fully quantum mechanical treatment of the interacting nanoparticle dimer.<sup>17,22</sup> Such linear quantum calculations have shown that for narrow junctions, electron tunneling across the junction can significantly reduce the plasmon-induced field enhancement.

In the present work, with example of a strongly coupled nanosphere dimer illuminated by a short laser pulse we show that electron current through the interparticle junction is highly nonlinear in the incident electric field strength. This results in nonlinear reduction of the plasmon-induced field enhancement

Received: November 2, 2011

Published: February 9, 2012

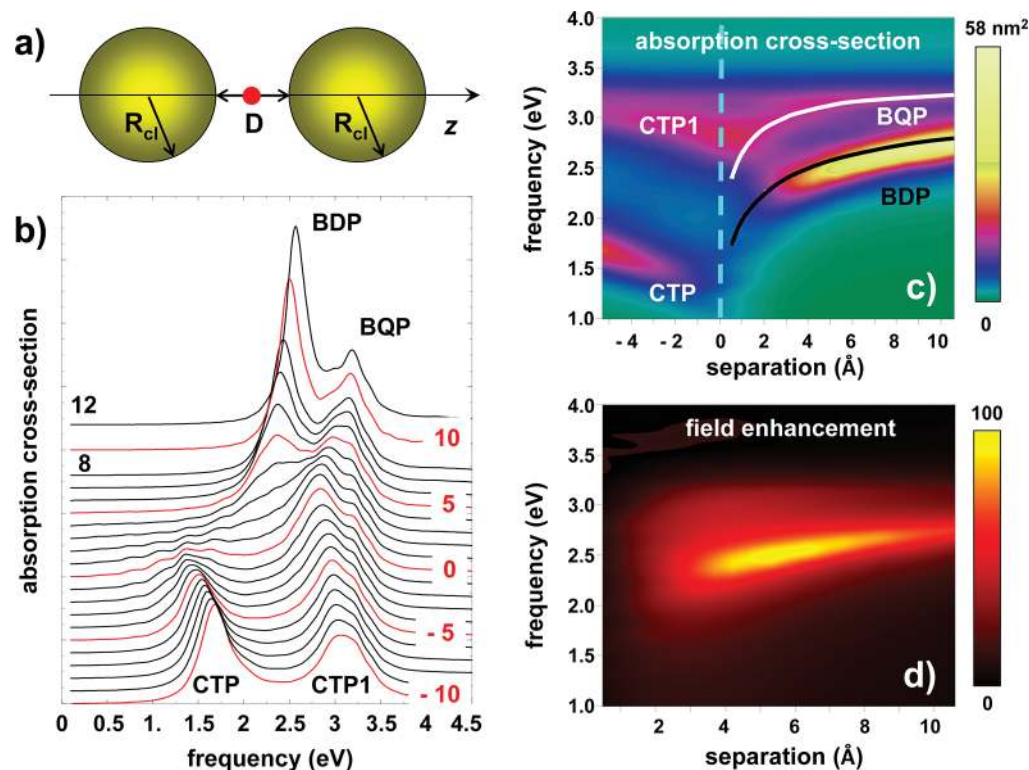


**Figure 1.** (a) Sketch of geometry of the nanoparticle dimer. The field enhancement is determined from the fields at the middle of the junction (red point). (b) Waterfall plot of the optical absorption cross-section. TDDFT results are given as function of the frequency  $\omega$  for different separations  $D$ . The  $D$ -values grow in steps of  $1 a_0 = 0.053$  nm, and the red curves labeled with corresponding  $D$ -values are used each  $5 a_0$  of  $D$ -change. The three topmost curves are obtained with  $D = 8, 10$  and  $12 a_0$ . The plasmonic modes responsible for the peaks in the absorption cross-section are indicated (see the text). (c) Contour plot of the optical absorption cross-section. TDDFT results are shown as function of the interparticle separation  $D$  and frequency  $\omega$ . White and red curves show the energies of the resonant absorption peaks in the classical calculations. Vertical blue line marks the contact point  $D = 0$ . The color scale is shown at the insert. (d) Calculated TDDFT field enhancement as function of the interparticle separation  $D$  and frequency  $\omega$ . The color scale is shown at the insert.

for moderate to large incident light intensities. The nonlinear effect is caused by the strong field photoemission because of the enhanced optical fields in the junction. The electrons are emitted from the surface of one nanoparticle, cross the junction and are injected into the other nanoparticle of the dimer. Increased (as compared to the linear regime) electronic current more efficiently neutralizes the charge densities on the opposite sides of the junction. Consequently, the electric field enhancement is reduced. The effect predicted here is a robust quantum mechanical phenomenon that appears for nanometer-sized junctions and that could be accessed experimentally by measuring a nonlinear optical signal such as SERS or four-wave mixing as a function of incident field strength.

Our model system is illustrated in Figure 1a where two identical spherical nanoparticles of radii  $R_{cl}$  are separated by a variable distance  $D$ . An atomistic description of the nanoparticles would severely limit the size of the system that can be treated quantum mechanically. As a consequence the collective plasmonic modes will be not well developed. We thus adopt the spherical jellium model (JM). Despite its simplicity, this model captures the collective plasmonic modes of the conduction electrons in individual nanoparticles and nanoparticle dimers.<sup>17,18,22,23</sup> The JM has also been successfully used to model effects associated with conduction electrons in a variety of metallic systems such as electronic and optical properties of metal clusters and surfaces,<sup>24–27</sup> charge transfer reactions between atoms and surfaces,<sup>28</sup> conductances of molecular junctions,<sup>29</sup> and strong-field effects.<sup>30</sup> While the JM obviously

does not provide chemical accuracy, it is well suited for the description of the novel physical effect predicted in the present paper, that is, an electric field-induced enhanced interparticle tunneling of conduction electrons across the junction of a strongly coupled nanoparticle dimer.

Within the JM the ionic cores of the nanoparticle atoms are represented with uniform background charge density  $n_+ = (4\pi r_s^3/3)^{-1}$ . The screening radius  $r_s$  is set equal to  $4 a_0$  (Bohr radius  $a_0 = 0.053$  nm) corresponding to Na metal that is a prototype system for the JM description. It should be emphasized that the qualitative conclusions drawn in this work are robust and independent of the particular choice of density parameter. This is further supported by comparing linear response results obtained here with those calculated previously with stabilized JM for gold.<sup>17</sup> Each of nanoparticles has a closed shell structure and consists of  $N_e = 1074$  electrons, so that the nanoparticle response exhibits a well-developed plasmon resonance. The sphere radius is  $R_{cl} = N_e^{1/3} r_s = 40.96 a_0 (\approx 2.17$  nm), and the Fermi energy of the system is at 2.9 eV below the vacuum level.

The time evolution of the electronic density  $n(\mathbf{r},t)$  in response to the external laser field is calculated ab initio within the Kohn–Sham (KS) scheme of the time-dependent density functional theory (TDDFT).<sup>31,32</sup> We use the adiabatic local density approximation (ALDA) with the exchange-correlation functional of Gunnarson and Lundqvist.<sup>33</sup> Retardation effects can be neglected due to the small size of the system. Our approach is described in details in the Supporting Information.

In order to understand the nonlinear effect, we first address the linear optical response. In Figure 1b,c, we show the calculated dipolar optical absorption cross-section of the metallic dimer. The TDDFT calculations have been performed for both positive and negative separations  $D$ , where the latter means a geometrical overlap between the particles. The  $D = 0$  case corresponds to touching jellium edges where the distance between the topmost atomic planes equals to the interlayer spacing, that is, a continuous solid is formed.

For large positive separations where interparticle electron tunneling is negligible, the TDDFT results agree with classical calculations marked with lines in Figure 1c. The absorption is dominated by the bonding dimer plasmon (BDP) originating from the hybridization of the dipolar plasmon modes of the individual nanospheres. The contribution from the higher frequency hybridized bonding quadrupolar (BQP) mode is also visible. As  $D$  decreases, the BDP and BQP modes red shift because of the interaction of surface charges on the opposite sides of the junction. The classical and quantum results differ at short separations because of electron tunneling between the nanospheres.<sup>17</sup> In the classical theory, the BDP and BQP modes exist down to the touching limit and experience a strong red shift. The quantum calculations show a progressive disappearance of the BDP mode prior to the direct contact between the nanoparticles ( $D = 0$ ). Similarly, prior to the direct contact, the spectral intensity is transferred from the BQP mode of the separated nanoparticles to the CTP1 mode. Here, CTP and CTP1 labels the charge transfer plasmon modes of the conductively coupled dimer.<sup>15,34–36</sup> The lowest CTP mode corresponds to a dipolar polarization with opposite charges at nanospheres, and the CTP1 mode is the next higher multipolar mode. The CTP mode appears as a broad shallow low-frequency peak at  $D = 0–0.1$  nm, and it evolves into a well-defined resonance at negative separations  $D < 0$ . For a dimer with well-established conductive contact, the CTP and CTP1 modes experience a classically predicted blue shift with increasing overlap between the nanospheres.<sup>15</sup>

In Figure 1d, we show the field enhancement in the center of the junction as obtained from the TDDFT calculations. For large separations, the optical fields are strongly enhanced at the dipolar plasmon resonance. Down to separation distances of  $D \approx 0.5$  nm, the field enhancement increases with decreasing  $D$ , which is in agreement with classical calculations. Below  $D \approx 0.5$  nm separation, because of the interparticle electron tunneling, the field enhancement decreases with decreasing  $D$ , and it is completely quenched close to the contact point.<sup>17</sup> Indeed, the tunneling probability increases with decreasing  $D$ , and the tunneling current flowing through the junction neutralizes the induced charges at its opposite sides. Thus, the quantum results show that there is no classically predicted  $1/D$  divergence of the fields<sup>15</sup> between the noncontact and contact regimes.

The finding that electron tunneling determines the optical response of a coupled nanoparticle dimer at small separations naturally leads to the question of possible strong field effects. Indeed, in the case of intense incident electromagnetic fields, further field enhancement in the junction due to the plasmonic excitation might drive the system to the optical field ionization regime. The electron current through the junction will then be increased, thus reducing the electric field enhancement. To check this idea, we have performed TDDFT calculations on the plasmonic dimer subjected to an incident  $z$ -polarized laser pulse with electric field given by  $E_L(t) = E_0 \exp[-(t-t_0)^2/T^2] \cos \Omega t$ . The frequency of the pulse  $\Omega$  has been set resonant with

the BDP. The duration of the pulse has been set to  $2T = 5.8$  fs, which is well below the characteristic times of energy transfer from excited electrons to phonons.<sup>30</sup> The integrated power  $\mathcal{P}$  of the pulse has been varied within a wide range of values of  $10^6–10^{12}$  W/cm<sup>2</sup> in order to probe both the linear and nonlinear strong-field regimes.

The field enhancement  $\mathcal{R} = E_{\max}/E_0$  with  $E_{\max}$  being the maximum value of the field reached in the middle of the junction during the irradiation time, is shown in Figure 2 for

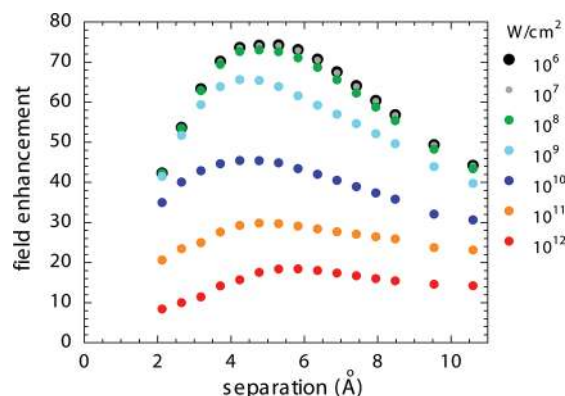


**Figure 2.** Field enhancement calculated in the middle of the junction for an incident pulse resonant with the bonding dimer plasmon BDP. TDDFT results are shown as function of the interparticle separation for different powers of the incident laser pulse (see the legend).

various values of the power of the incident laser pulse  $\mathcal{P}$ . Results are presented for interparticle separations ranging from  $D = 1$  nm down to  $D = 0.2$  nm. Shorter distances are not shown because the BDP mode is then not well-defined. (see Figure 1b,c). For weak pulses the system responds linearly with field enhancement in the junction being independent of  $\mathcal{P}$ . For incident power of  $\mathcal{P} = 10^9$  W/cm<sup>2</sup>, nonlinear effects appear and become pronounced for higher laser powers. The field enhancement in the junction decreases with increasing  $\mathcal{P}$ . For the most intense pulse  $\mathcal{P} = 10^{12}$  W/cm<sup>2</sup>, the field enhancement is five times smaller than in the linear regime. We note that the nonlinear behavior is present for the entire range of interparticle separations studied.

To obtain further insights into the origin of the nonlinear effect, we analyze the time evolution of the induced currents and fields. Figure 3 summarizes the results for a dimer with separation distance of  $D = 6 a_0$  (0.32 nm). Figure 3a shows the instantaneous current  $I$  through the  $(x,y)$  plane in the middle of the junction, and Figure 3b shows the local electric field in the center of the junction (i.e., measured at  $D/2$  on the  $z$ -axis). The results are normalized to the amplitude  $E_0$  of the incident pulse. For incident powers up to  $\mathcal{P} = 10^8$  W/cm<sup>2</sup> the system responds linearly with maximum field enhancement of the order of 60, and the scaled tunneling currents (fields) follow the same curve for different  $\mathcal{P}$ . The tunneling current is in phase with the local electric field showing a resistive response of the junction.

When the power of the incident pulse is raised above  $10^9$  W/cm<sup>2</sup> nonlinear effects become visible. The scaled current  $I/E_0$  between the nanospheres strongly increases. Since the current through the junction tends to neutralize the charges at its opposite sides, an increase of the scaled current leads to a smaller field enhancement. Two physical phenomena cause the increased conductivity of the junction at high laser powers. (i) The incident pulse excites conduction electrons in the individual nanoparticles.

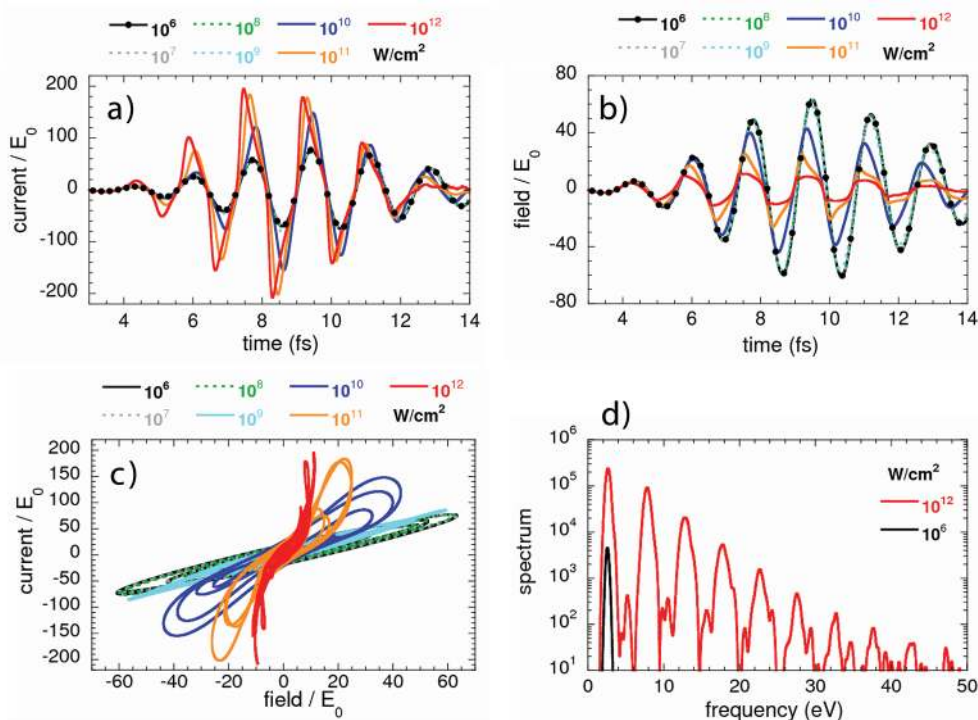


**Figure 3.** Detailed analysis of the currents and fields for interparticle separation  $D = 6a_0$  (0.32 nm). (a) Current through the junction as a function of time measured in femtoseconds (fs). Results are normalized to the amplitude  $E_0$  of the incident laser pulse. The data are shown for the 2.4–14.3 fs time interval when the incident laser pulse impinges on the system. The insert relates the different colors/symbols used with the power  $\mathcal{P}$  of the incident pulse. (b) The same as panel a but for the electric field in the middle of the junction. (c) Normalized current through the junction plotted as a function of the normalized electric field in the middle of the junction. Different colors are explained in the insert. (d) Fourier analysis of the current  $I(t)$  through the junction.  $\omega^2 I(\omega)^2$  is shown for the smallest and largest power of the incident pulse as calculated here.

Such “hot” electrons experience a lower tunneling barrier and can therefore more easily tunnel between the two particles. (ii) The strong local fields in the junction reduce the potential barrier between the nanoparticles and drive the system toward a nonlinear optical field emission regime.

The nonlinearity is clearly observed in Figure 3a,b for  $\mathcal{P} = 10^{12}$  W/cm<sup>2</sup>. During the optical semiperiod, the rise in the local field in the junction leads to an abrupt nonlinear increase of the current, which neutralizes the charges at opposite sides of the junction so that the field saturates. During the next semiperiod, the situation is repeated but with currents and electric fields in the opposite direction. The calculations show that for the strongest pulse  $\sim 23$  electrons can be transferred across the junction during a half-period for  $D = 6 a_0$  (0.32 nm), and  $\sim 12$  electrons are transferred for  $D = 20 a_0$  (1.06 nm). This explains the reduction of the field enhancement.

It is noteworthy that the onset of the strong field effects observed here at  $\mathcal{P} = 10^9$  W/cm<sup>2</sup> is consistent with experimental findings for sharp metal tips, where the onset of strong field effects was reported for laser intensities of  $\mathcal{P} = 10^{11}$  W/cm<sup>2</sup>.<sup>37–39</sup> Indeed, for the present system the field enhancement in the junction of the dimer is of the order of 40 for  $\mathcal{P} = 10^9$  W/cm<sup>2</sup>, while for a tip, a lower (4 to 8 times) field enhancement has been estimated.<sup>38,39</sup> The order of magnitude difference in the field enhancement between the dimer and the tip results in 2 orders of magnitude difference in the intensity of the incident laser pulse required to reach equivalent fields at the surface.

The transition from linear to nonlinear behavior can be clearly observed in Figure 3c. The current  $I(t)$  between the nanoparticles is shown as a function of the field  $E(t)$  in the middle of the junction for the 2.4–14.3 fs time interval. At low incident

power, the resistive nature of the junction implies a relation  $I(t) = \sigma E(t)$  between the current and the local field. In the linear regime,  $\sigma$  is independent of the incident laser power  $\mathcal{P}$ . At intermediate laser power the proportionality between  $I(t)$  and  $E(t)$  still provides a reasonable description of the calculated results, but with an increasing  $\sigma = dI/dE$ . This can be ascribed to the excitation of hot electrons which experience a lower tunneling barrier. At high  $\mathcal{P} = 10^{12}$  W/cm<sup>2</sup>, the nonlinear discharge between the nanoparticles appears as a divergence in  $dI/dE$ , that is, small change in the field leads to the strong increase of the tunneling current.

The nonlinear response of the system results in the generation of high harmonic currents, as shown in Figure 3d. A Fourier analysis of the current  $I(t)$  reveals that in the linear regime ( $\mathcal{P} = 10^6$  W/cm<sup>2</sup>) there is only signal at the frequency of the incident pulse  $\Omega$ . In contrast, for large power  $\mathcal{P} = 10^{12}$  W/cm<sup>2</sup>, odd higher harmonics  $(2m + 1)\Omega$ , ( $m = 1, 2, 3, \dots$ ) appear in the spectrum. Because of the symmetry, even harmonics are suppressed, similar to the experimental observations of high harmonic generation in different plasmonic structures.<sup>40–42</sup> However, the “conventional” nonlinearity addressed in these previous works is due to transitions between the electronic bands within the nanostructures. The field enhancement provided by a dimer configuration has been previously discussed only as a way to increase the local intensity of the incident light which enables high harmonic generation.<sup>12,40–43</sup> Here we show that for the small separations a plasmonic dimer exhibits an additional nonlinear effect. This effect is linked with interparticle transfer of conduction electrons and results in a reduction of the field enhancement. Since an oscillating current will radiate at its oscillation frequencies, the dimer will emit light at high harmonics. A detailed investigation of the cross

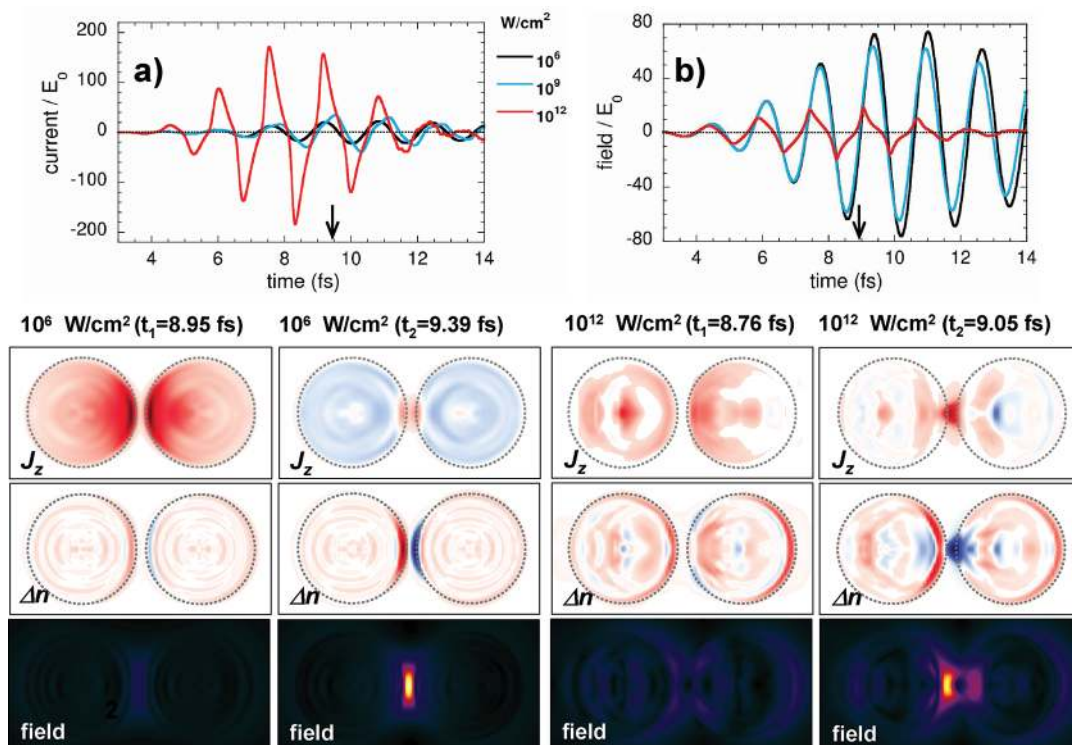


**Figure 4.** Time evolution of the induced currents, charge densities and fields for interparticle separation  $D = 10 a_0$  (0.53 nm). (a,b) Same as Figure 3 but for  $D = 0.53$  nm. Lower panels show the snapshots of the induced z-component of the current density  $J_z(t)$ ; induced charge density  $\Delta n(t)$ ; and the field intensity  $|E|$ . Results are shown in the  $(x,z)$  plane for both; the linear response regime with power of the incident pulse  $\mathcal{P} = 10^6$  W/cm<sup>2</sup> and for the nonlinear regime with  $\mathcal{P} = 10^{12}$  W/cm<sup>2</sup>. To show the pertinent details we use different color scales for low and high power of the incident pulse. Red (blue) color is used for the positive (negative) values of the induced currents and charges. The instances of time  $t_1$  ( $t_2$ ) when the field in the middle of the junction is close to minimum (maximum) are picked as times around the time  $t = 9$  fs as indicated by arrows in panels a and b.

section for high harmonic generation and its comparison with cross section for the "conventional" nonlinearity is beyond the scope of the present paper.

Figure 4 further illustrates the dynamics of the charges and fields in the dimer. The results are presented for dimer separation of  $D = 10 a_0$  (0.53 nm) where the tunneling conductance in the linear regime is low. Consequently, the nonlinear enhancement of the tunneling current seen in panel a is much more pronounced than for  $D = 6 a_0$  (0.32 nm) in Figure 3a. The field dynamics shown in panel b is similar to that of Figure 3b with a nonharmonic time evolution of the fields at high power of the incident pulse and with field enhancement reduced by the nonlinear effect.

The lower panels of Figure 4 show snapshots of the z-component of the current density, induced charge density, and the field intensities for the linear and nonlinear regimes. The instances of time ( $t_1$ ) and ( $t_2$ ) are picked within 1/4 optical period where the field in the junction passes through its minimum ( $t_1$ ) or maximum ( $t_2$ ) values. In both the linear and nonlinear regimes, at  $t_1$  the induced charges at the surfaces of nanoparticles are small. The large positive current inside each nanoparticle moves the charges toward the surface and creates a dipolar polarization consistent with resonant excitation of the BDP. In the linear regime,  $t_2$  corresponds to a fully developed induced dipole. Thus, the current inside nanoparticles is close to zero, and a large charge density is induced at surfaces of the nanoparticles in particular at the opposite sides of the junction. The current and electric field at  $t_2$  appear strikingly different in the nonlinear regime. The high field in the junction leads to electronic discharge which appears as strong positive current

across the junction. This effect also manifests itself as large negative charge density (electrons) in the junction, as displayed in the right most panel in Figure 4. The current neutralizes the induced charges at opposite sides of the junction and consequently reduces the field and modifies its spatial profile.

Several comments are in order regarding approximations used in this work. While the JM description is well suited for the Na nanoparticles as the ones discussed here, noble metal nanoparticles can present additional effects not accounted for within the JM. In particular, even though delocalized and less bound sp-band electrons might be assumed to give the dominant contribution to the field emission current, the contribution from the localized d-electrons can not be excluded. Furthermore, nonlinear effects linked with interband transitions within the nanoparticles may be important and are not adequately included in the JM. The present calculation was based on the local density approximation so that the electron image potential outside the surface is not reproduced. The tunneling barrier between the two nanoparticles is thus overestimated leading to an underestimate of the distances where tunneling effects become important.<sup>17</sup>

While the present calculations have been performed for very small systems, the results are robust and caused by universal quantum mechanical phenomena such as electron tunneling and electron hole pair excitation. The size of individual particles is sufficient for their optical spectra to exhibit well-developed plasmon resonances and hybridized modes as depicted in Figure 1, and as is typically observed for larger systems. The tunneling phenomena that cause the nonlinear effects reported here depend on the local electron potential barrier separating

the two ground-state nanoparticles and on the field in the junction. The potential barrier does not depend on the size of the nanoparticles but on the width of the junction. At the same time, the plasmon-induced electric field is size-dependent and will increase for larger nanoparticles for a fixed junction width. Thus we expect that the proposed nonlinear effects will occur for lower light intensities in the case of dimers consisting of particles of radii of larger than those considered here (see also ref 12). For large systems, however, retardation effects can play a role modifying the plasmonic response and thus the fields in the junction.

In conclusion, we have presented a fully quantum mechanical study of nonlinear effects in a plasmonic nanosphere dimer. The time-dependent density functional theory has been used to investigate the dynamics of the electronic response of the system and to calculate the field enhancement as a function of the interparticle separation and power of the incident laser pulse. We have found that for moderate and strong laser pulses, excitation of the conduction electrons and plasmonic field enhancement in the junction drives the system into the field emission regime. The increased electron current neutralizes the charge densities on the opposite sides of the junction. We find that the nonlinear current through the junction can be established even for interparticle separations of 1 nm where electron tunneling between the particles is negligible in the linear response case. Consequently, the electric field in the junction is strongly reduced as compared to the predictions derived from pure linear theory. The reduction of the local field enhancement can reach a factor of 5 for the most intense  $10^{12}$  W/cm<sup>2</sup> laser pulse considered here. The effect reported here is essentially a nonlinear phenomenon that depends on the intensity of the incoming radiation. It should be taken into account when designing nanoplasmonic devices based on plasmon-induced field enhancement effect.

## ■ ASSOCIATED CONTENT

### Supporting Information

Details on the TDDFT calculations. Classical calculation of the optical response of the nanoparticle dimer. Field enhancement of the nanoparticle dimer. Density dynamics. This material is available free of charge via the Internet at <http://pubs.acs.org>.

## ■ AUTHOR INFORMATION

### Corresponding Author

\*E-mail: [andrei.borissov@u-psud.fr](mailto:andrei.borissov@u-psud.fr).

### Notes

The authors declare no competing financial interest.

## ■ ACKNOWLEDGMENTS

A.G.B. gratefully acknowledges enlightening discussions with J.-P. Gauiyacq. J.A. acknowledges financial support from the Department of Industry of the Basque Government through the ETORTEK project nanoiker, the Spanish Ministerio de Ciencia e Innovación through Project No. FIS2010-19609-C02-01 and Project No. EUI2008-03816 CUBIHOLE from the Internationalization Program. P.N. acknowledges support from the Robert A. Welch Foundation (C-1222) and the Office of Naval Research (N00014-10-1-0989).

## ■ REFERENCES

(1) Kelly, L.; Coronado, E.; Zhao, L. L.; Schatz, G. C. *J. Phys. Chem. B* **2003**, *107*, 668.

- (2) Alvarez-Puebla, R.; Liz-Marzán, L. M.; García de Abajo, F. J. *J. Phys. Chem. Lett.* **2010**, *1*, 2428.
- (3) Schuller, J. A.; Barnard, E. S.; Cai, W.; Jun, Y. C.; White, J. S.; Brongersma, M. L. *Nat. Mater.* **2010**, *9*, 193.
- (4) Halas, N. J.; Lal, S.; Chang, W.-S.; Link, S.; Nordlander, P. *Chem. Rev.* **2011**, *111*, 3913.
- (5) Pasquale, A. J.; Reinhard, B. M.; Negro, L. D. *ACS Nano* **2011**, *5*, 6578.
- (6) Xu, H.; Bjeneld, E.; Käll, M.; Börjesson, L. *Phys. Rev. Lett.* **1999**, *83*, 4357.
- (7) Talley, C. E.; Jackson, J. B.; Oubre, C.; Grady, N. K.; Hollars, C. W.; Lane, S. M.; Huser, T. R.; Nordlander, P.; Halas, N. J. *Nano Lett.* **2005**, *5*, 1569.
- (8) Theiss, J.; Pavaskar, P.; Echternach, P. M.; Muller, R. E.; Cronin, S. B. *Nano Lett.* **2010**, *10*, 2749.
- (9) Mühlischlegel, P.; Eisler, H.-J.; Martin, O. J. F.; Hecht, B.; Pohl, D. W. *Science* **2005**, *308*, 1607.
- (10) Bharadwaj, P.; Deutsch, B.; Novotny, L. *Adv. Opt. Photonics* **2009**, *1*, 438.
- (11) Taminiou, T. H.; Stefani, F. D.; Segerink, F. B.; van Hulst, N. F. *Nat. Photonics* **2008**, *2*, 234.
- (12) Kim, S.; Jin, J.; Kim, Y.-J.; Park, I.-Y.; Kim, Y.; Kim, S.-W. *Nature* **2008**, *453*, 757–760.
- (13) García-Martín, A.; Ward, D. R.; Natelson, D.; Cuevas, J. C. *Phys. Rev. B* **2011**, *83*, 193404.
- (14) Hao, E.; Schatz, G. C. *J. Chem. Phys.* **2004**, *120*, 357.
- (15) Romero, I.; Aizpurua, J.; Bryant, G. W.; García de Abajo, F. J. *Opt. Express* **2006**, *14*, 9988.
- (16) Jain, P. K.; El-Sayed, M. A. *Chem. Phys. Lett.* **2010**, *487*, 153.
- (17) Zuolaga, J.; Prodan, E.; Nordlander, P. *Nano Lett.* **2009**, *9*, 887.
- (18) Zuloaga, J.; Prodan, E.; Nordlander, P. *ACS Nano* **2010**, *4*, 5269.
- (19) García de Abajo, F. J. *J. Phys. Chem. C* **2008**, *112*, 17983.
- (20) McMahon, J. M.; Gray, S. K.; Schatz, G. C. *Phys. Rev. Lett.* **2009**, *103*, 097403.
- (21) McMahon, J. M.; Gray, S. K.; Schatz, G. C. *Nano Lett.* **2010**, *10*, 3473.
- (22) Mao, L.; Li, Z.; Wu, B.; Xu, H. *Appl. Phys. Lett.* **2009**, *94*, 243102.
- (23) Townsend, E.; Bryant, G. W. *Nano Lett.* **2012**, *12*, 429.
- (24) Ekardt, W. *Phys. Rev. B* **1985**, *31*, 6360.
- (25) de Heer, W. A.; Milani, P.; Châtelain, A. *Phys. Rev. Lett.* **1989**, *63*, 2834.
- (26) Hervieux, P.-A.; Bigot, J.-Y. *Phys. Rev. Lett.* **2004**, *92*, 197402.
- (27) Prodan, E.; Nordlander, P.; Halas, N. J. *Nano Lett.* **2003**, *3*, 1411–1415.
- (28) Winter, H. *Phys. Rep.* **2002**, *367*, 387.
- (29) Lang, N. D.; Avouris, P. *Nano Lett.* **2002**, *2*, 1047.
- (30) Fennel, Th.; Meiwes-Broer, K.-H.; Tiggesbäumker, J.; Reinhard, P.-G.; Dinh, P. M.; Suraud, E. *Rev. Mod. Phys.* **2010**, *82*, 1793.
- (31) Marques, M. A. L.; Gross, E. K. U. *Annu. Rev. Phys. Chem.* **2004**, *55*, 427–455.
- (32) Stratmann, R. E.; Scuseria, G. E.; Frisch, M. J. *J. Chem. Phys.* **1998**, *109*, 8218.
- (33) Gunnarson, O.; Lundqvist, B. I. *Phys. Rev. B* **1976**, *13*, 4274.
- (34) Atay, T.; Song, J.-H.; Nurmikko, A. V. *Nano Lett.* **2004**, *4*, 1627.
- (35) Marhaba, S.; Bachelier, G.; Bonnet, Ch.; Broyer, M.; Cottancin, E.; Grillet, N.; Lerme, J.; Vialle, J.-L.; Pellarin, M. *J. Phys. Chem. C* **2009**, *113*, 4349.
- (36) Ćirić, S. S.; Kreuzer, M. P.; González, M. U.; Quidant, R. *ACS Nano* **2009**, *3*, 1231.
- (37) Yanagisawa, H.; Hafner, C.; Doná, P.; Klöckner, M.; Leuenberger, D.; Greber, T.; Hengsberger, M.; Osterwalder, J. *Phys. Rev. Lett.* **2009**, *103*, 257603.
- (38) Schenk, M.; Krüger, M.; Hommelhoff, P. *Phys. Rev. Lett.* **2010**, *105*, 257601.
- (39) Bormann, R.; Gulde, M.; Weismann, A.; Yalunin, S. V.; Ropers, C. *Phys. Rev. Lett.* **2010**, *105*, 147601.
- (40) Danckwerts, M.; Novotny, L. *Phys. Rev. Lett.* **2007**, *98*, 026104.

(41) Hanke, T.; Krauss, G.; Trutlein, D.; Wild, B.; Bratschitsch, R.; Leitenstorfer, A. *Phys. Rev. Lett.* **2009**, *103*, 257404.

(42) Paloma, S.; Danckwerts, M.; Novotny, L. J. *Opt. A: Pure Appl. Opt.* **2009**, *11*, 114030.

(43) Cai, W.; Vasudev, A. P.; Brongersma, M. L. *Science* **2011**, *333*, 1720.